JOURNAL OF MATERIALS SCIENCE 27 (1992) 5831–5836

Jetting and fibre degradation in injection moulding of glass-fibre reinforced polyamides

M. AKAY, D. BARKLEY
Department of Mechanical and Industrial Engineering, University of Ulster at Jordanstown, Newtownabbey, County Antrim, BT37 OQB, UK

Injection-moulded glass fibre-reinforced polyamides with up to 50% by weight fibre content were examined for processing behaviour such as jetting and fibre degradation. Jetting was found to be a function of the ratio of the gate depth to mould-cavity depth, fibre length, fibre content and injection ram speed. Contrary to expectation, jetting occurred less frequently as the injection ram speed was increased. Major fibre degradation was experienced during the transport of the melt from the injection machine to the mould cavity. Further fibre degradation due to increases in injection back-pressure was comparatively small. Tensile strength was shown to be sensitive to variations in the fibre length distribution, whereas the elastic modulus remained unaffected.

1. Introduction

The ability to process fibre-reinforced thermoplastic granules with conventional injection-moulding equipment is most convenient. However, certain precautions must be taken to achieve potential advantages offered by these materials. Processing and tool parameters appropriate for the base polymer will not necessarily yield best results in the fibre-reinforced grades. Rules governing the processing behaviour of thermoplastics ought to be verified with fibre incorporation, particularly as fibre length and/or fibre content increases. Accordingly the work reported here examined injection-moulded short (< 1 mm) and long glass fibre (< 10 mm) reinforced polyamides with up to 50% by weight fibre content and attempted to inter-relate process and tool variables, jetting, fibre-length distribution and tensile properties.

Jetting is an initial pencil-like narrow stream of melt which is usually followed by an expanding melt front, causing it to fold and gather up wholly or partially at the opposite end of the mould. It is associated with extrudate (die) swell and is likely to occur [1] when the depth of the meltstream emerging from the gate is less or equal to the cavity depth. Extrudate swelling is related to the ability of the polymer to undergo elastic strain recovery. Thus an increased melt strain within the die results in increased extrudate swell. At higher injection speeds, because of the associated increase in shear rate, the swelling ratio increases [2] and, therefore, jetting becomes less likely. However, at very high shear rates the combination of pseudoplastic behaviour and adiabatic heating can reduce the viscosity sufficiently enough to limit the swell and hence cause jetting. As would be expected, the addition of rigid particulate and/or fibre fillers reduces extrudate swell and causes jetting [3, 4] although it has also been shown [4] that the inclusion of long-glass fibres ($\geq$ 5 mm) can result in large die swells depending on the die geometry.

The moulding and fabrication processes degrade the original fibre length of the raw material and, as a result, all discontinuous fibre-reinforced parts contain a distribution of fibre lengths. The effective fibre length needed for matrix to fibre stress transfer, l_{tr}, under tension and parallel to the fibre direction, varies with strain, ε, such that $l_{tr} = (\varepsilon E r)/\tau$, where E is the elastic modulus of fibre, r the radius and τ the interfacial shear strength. At fibre fracture, l_{tr} reaches a maximum value known as the critical fibre length, l_c. It becomes necessary to sum the strength contributions of all fibres shorter than l_{tr} (subtransfer) and all fibres longer than l_{tr} (supratransfer). At low strains, when l_{tr} is small, most of the fibres are supratransfer but, as the strain increases, an increasing proportion of the fibres will become subtransfer. Consequently, the fibre-reinforcement efficiency will be high at low strains but will deteriorate as the strain increases (see Reference 5 for further details).

2. Experimental procedure

The materials used are detailed in Table I.

The raw materials were dried in a vacuum oven at 95 °C for 4 h prior to processing. Mouldings were prepared in the form of plaques of $2 \times 120 \times 120$ mm^3 using a Stubbe SKM51 injection-moulding machine, rated at 500 kN clamp force and 70 ml shot volume. The machine was set at 13 MPa hydraulic pressure, 80 rev min^{-1} screw speed, 0.7 or 1.7 MPa back pressure, 25 or 50 mm s^{-1} ram forward speed, 20 s

0022–2461

TABLE I Raw materials

Description	Identification	ICI grade
Unfilled polyamide	PA	Maranyl A100
30% short glass fibre-reinforced polyamide	SFRPA30	Maranyl A175
50% short glass fibre-reinforced polyamide	SFRPA50	Maranyl A690
50% long glass fibre-reinforced polyamide	LFRPA50	Verton RF 70010

cooling time, barrel temperature profile of 260, 270, 280, 290 °C, and 80 °C mould temperature. The mouldings were placed in sealed impermeable bags with silica-gel desiccant, until required for testing.

The mould was designed and manufactured with the options of filling from any combination of five variable axis gates of variable dimensions (Fig. 1). It has cylindrical sockets of 20 mm diameter for the gates to insert. A range of inserts enable gate dimensions (width × depth) of 2×2, 4×0.5, 4×1, 4×1.5, 4×2, 6×0.5, 6×1, 6×1.5 and 6×2 mm^2. The diameter of the sprue is approximately 6 mm. In this study, only one of the gate positions, see Fig. 2, was used. A series of short-shot mouldings were produced without mould release agent, to examine mould-filling behaviour.

The fibre-length distributions were obtained by adopting a technique [6] based on separation of fibres into different lengths by sieving. Initially the fibres were extracted by burning off the polymer in a furnace for 1 h at 600 °C. Approximately 50 mg fibre residue was dispersed in water using an ultrasonic water bath shaker. The mixture of dispersed fibres was decanted into a stack of sieves which were already filled with water. The stack includes, eight sieves of 4, 2.8, 1.4 mm and 710, 300, 150, 45 μm apertures arranged in descending order from the top. The bottom container of the stack has a small (1 mm diameter) hole which allowed the water to run. Care was taken to maintain a constant water level during the decanting. Once the stack had completely drained, the contents of each sieve were flushed into a set of dishes. These dishes were fabricated from a flat glass plate ($100 \times 127 \times 1.5$ mm^3) to which a circular perspex rim (50 mm diameter and 13 mm height) was glued. These dimensions were chosen so that the dishes would fit in the negative carrier of a Blumfield enlarger. Thus prints of the fibres ($\times 4$ magnification) contained in the dishes could be obtained directly from the enlarger. These prints were placed on a digital tablet and approximately 1000 fibres were digitized under a magnifier. Using fibre analysis software, a histogram of the fibre lengths could then be drawn.

Tensile tests were conducted in accordance with ASTM D638M, at 5 mm min^{-1}, employing an Instron-6025 tensile tester. Dumb-bell-shaped specimens were cut with a high-speed router longitudinal to the mould-fill direction and representing a location as shown in Fig. 3, because this is the maximum fibre-alignment region, where the fibres are predominantly parallel to the mould-fill direction for both the material systems [7]. The tests were conducted at room temperature and the results quoted represent an average of at least five measurements. The moisture content of the testpieces was determined by weighing before and after drying under vacuum at 80 °C for 24 h; indicating approximately 0.4% and 0.2% moisture in unfilled and filled grades, respectively.

3. Results and discussion

3.1. Jetting

The occurrence of jetting was examined under various process conditions and mould-gate dimensions. Jetting, depicted in Fig. 4, was not experienced with the unfilled polyamide and SFRPA30; however, the rest of the reinforced grades, with higher percentage of fibre contents, exhibited varying tendencies to jet as detailed in Table II.

A criterion [1] for jetting as (die swell ratio) × (mould-gate depth) ≤ (mould-cavity depth), had only a limited degree of application with the gate arrangement considered here, where one surface of the gate was maintained flush with the surface of the cavity. Short glass fibre-reinforced polyamides at shear rates encountered in injection-mould gates ($> 10^4$ s^{-1}) have been shown to exhibit swelling ratios less than one [4]. Therefore, according to the above criterion when the gate depth is less than or equal to the cavity depth, jetting should ensue. No jetting was observed with any of the materials when the mould was fitted with gates of 2 or 1.5 mm depths. At the reduced gate depth of 1 mm only the 50% glass fibre-reinforced polyamides jetted and LFRPA50 only at the lower injection speed of 25 mm s^{-1}. At higher injection speeds because of the associated increase in shear rate and molecular orientation, the gate swell increases and jetting is suppressed, although the associated reduction in viscosity might eventually reduce the relaxation time (viscosity/elastic modulus) sufficiently so that the melt strain could be relieved without excessive gate swell. Hence, very high shear rates (at injection speeds greater than employed here) may promote jetting.

The occurrence of any jetting in LFRPA50 is surprising because of the tendency of long fibre/polymer melt to expand in diverging flows. This can be demonstrated by free-space injections, see Fig. 5, where the fracture (burst) of the melt into tangled up strands upon release of strain energy on emergence from a constrained environment, such as the sprue, is in evidence. The expansion should enable contact to be maintained with the mould surface, and reduce the possibility of jetting. However, at this high fibre content, there is less polymer to ensure the initial wetting-out of the mould surface and hence to hinder the solid fibres from gliding along. Likewise, it must be noted that mould release-agent aids jetting [8] by reducing the degree of contact between the mould and the melt. Distortion of incident jet of melt upon solidifying, Fig. 6, may contribute to the establishment of contact between the ensuing melt and the mould surfaces and therefore curtail jetting. This, perhaps, is one of the

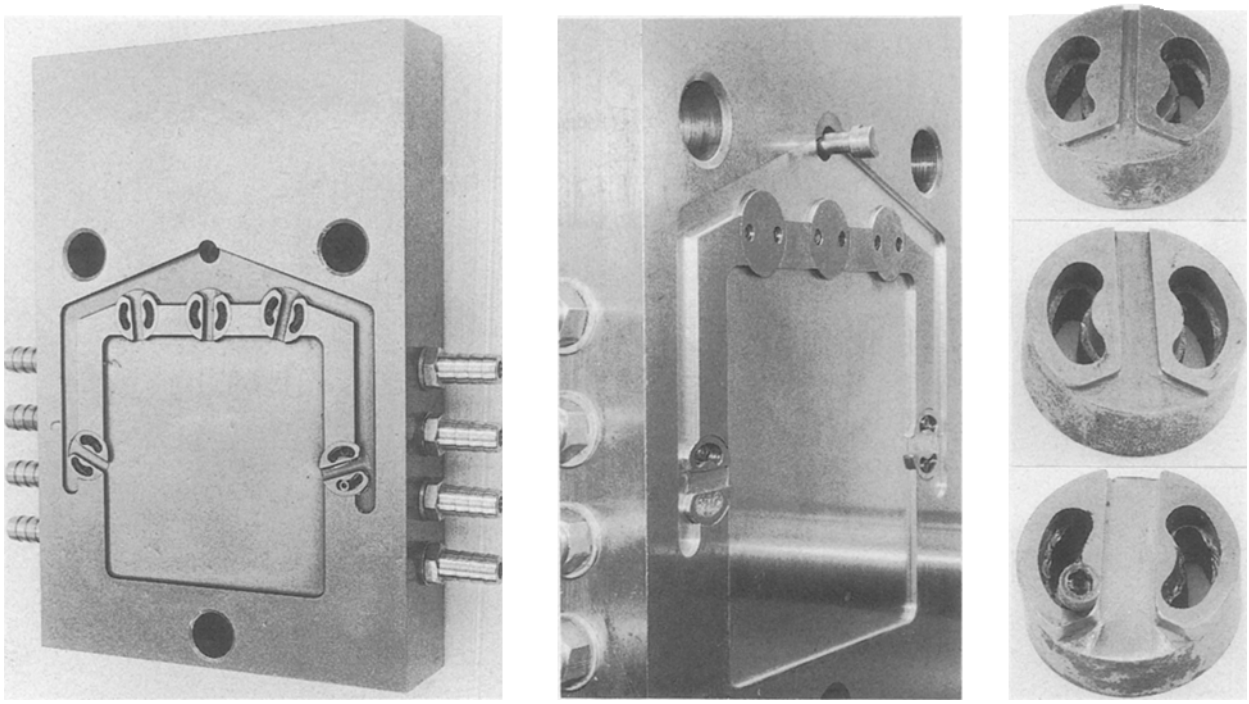

Figure 1 The mould with variable axis/geometry gates.

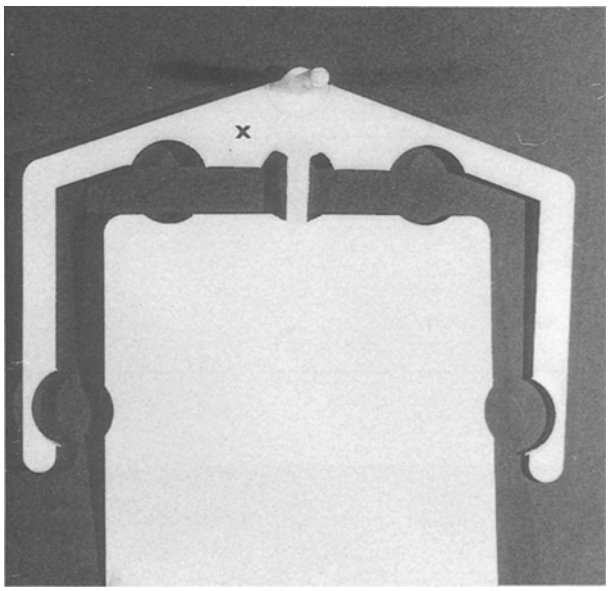

Figure 2 A typical moulding.

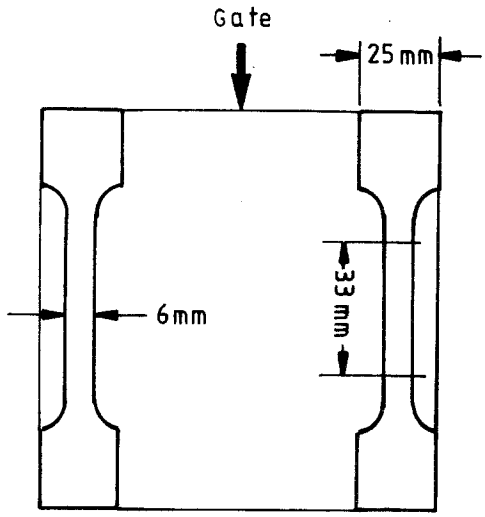

Figure 3 Details of tensile specimens.

reasons why jetting was not observed when the gate depth was only reduced from 2 mm to 1.5 mm.

3.2. Fibre degradation

To assess the effects of the various process parameters on the fibre lengths, a series of fibre-length distributions were obtained (Figs 7 and 8). Fig. 7 shows the distributions for a SFRPA50 plaque moulded at a back pressure of 0.7 MPa using two gate sizes (6×2 mm^2 and 6×1 mm^2). The distribution of the granule is included for comparison. It is considerably broader than the distributions from the processed samples. The effect of back pressure and smaller gate is to cause fibre damage which manifests itself as a reduction in both the average fibre length and the distribution width. In the case of the long-fibre grade this reduction in fibre length is drastic (Fig. 8). The LFRPA50 granule had almost all its fibres contained in a peak centred at 9 mm fibre length, the processed samples have peaks centred on 0.4 mm and contain no fibres longer than 6 mm.

Table III presents the UTS and elastic modulus values for different back pressures and gate dimensions. The UTS decreased by approximately 6% for SFRPA50 and 8% for LFRPA50 as the gate size was decreased or as the back pressure was increased. The corresponding changes in the elastic modulus were negligible. This may be explained in terms of the subtransfer and supratransfer fibre length fractions at different strain levels. Table IV provides the relevant information, extracted from the fibre-length

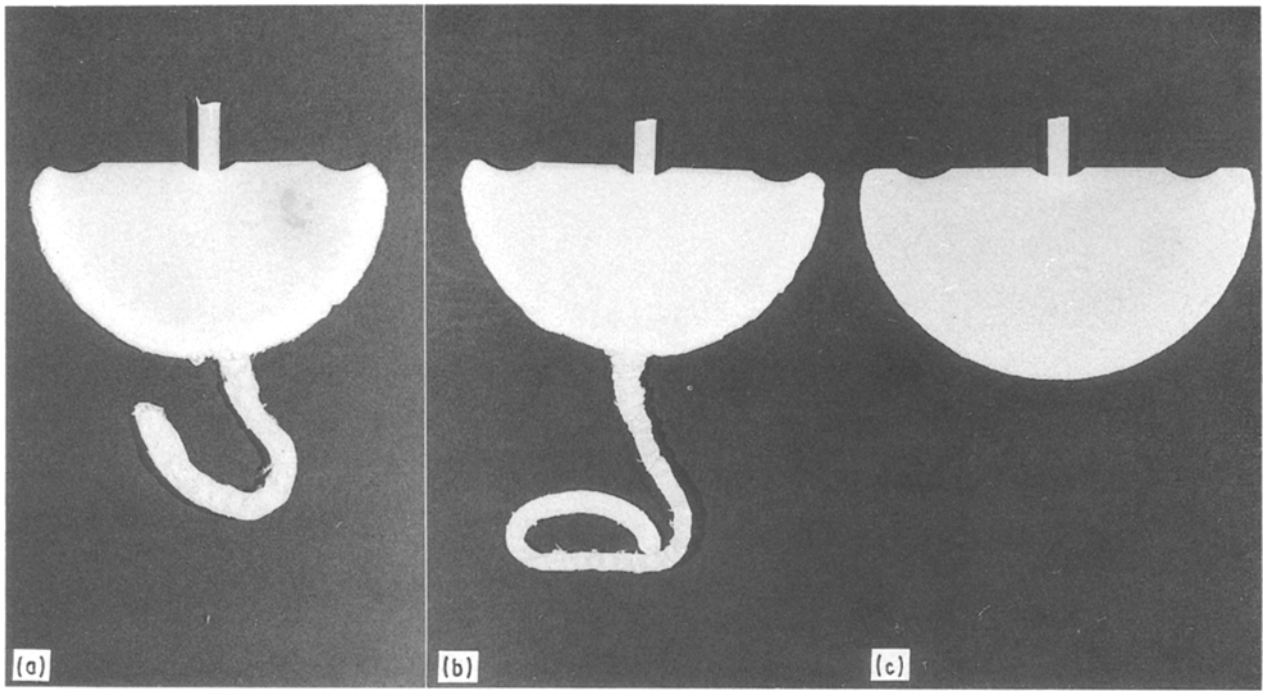

Figure 4 Short-shot mouldings for (a) LFRPA50, (b) SFRPA50, (c) SFRPA30.

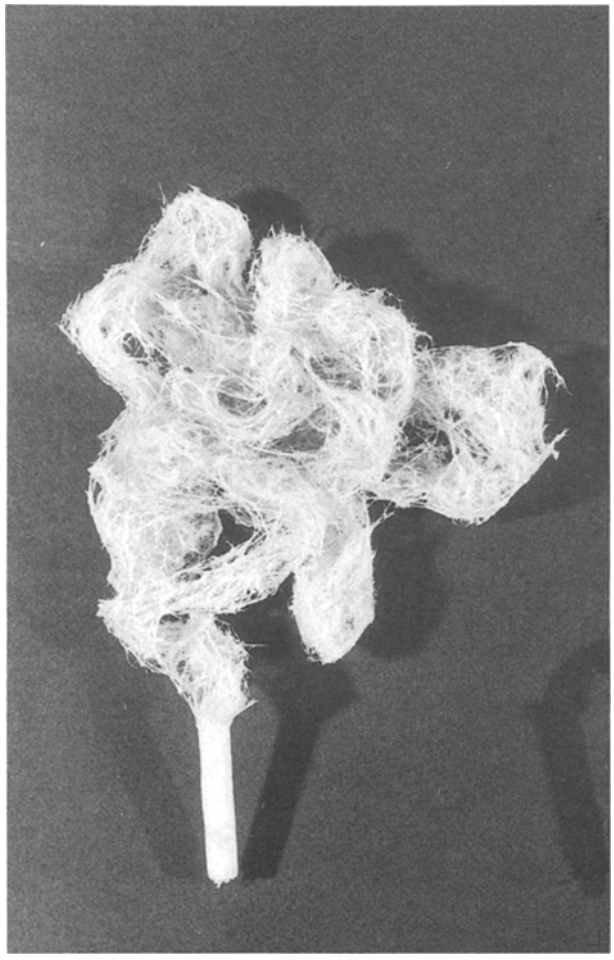

Figure 5 Free-space injection of LFRPA50 from the sprue.

TABLE II Frequency of jetting with a 6×1 mm^2 gate (representing ten observations for each condition)

Material	Injection ram speed (mm s^{-1})	Per cent jetted
PA	25	0
PA	50	0
SFRPA30	25	0
SFRPA30	50	0
SFRPA50	25	70
SFRPA50	50	60
LFRPA50	25	50
LFRPA50	50	0

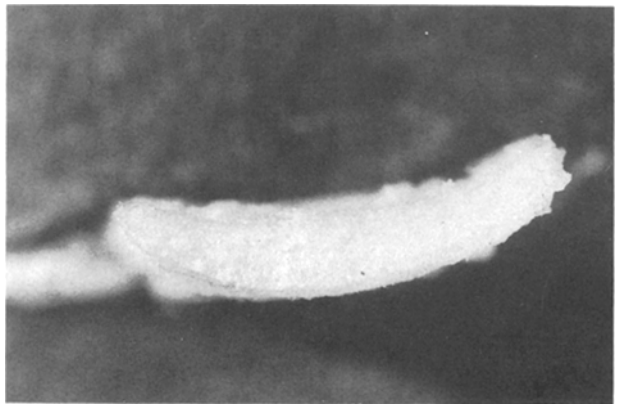

Figure 6 Cross-section of the tip of the jetting showing U-shaped distortion.

distributions. The data for the determination of the stress-transfer fibre lengths are also included in the table.

The values of l_{tr} increase as the strain increases, hence progressively more fibres become subtransfer and therefore less efficient as reinforcement. One implication of this strain dependence is that although strength is closely related to fibre-length distribution, stiffness is much less so. Elastic modulus is measured in the initial linear region of the stress/strain curve and this corresponds to low strains where nearly all

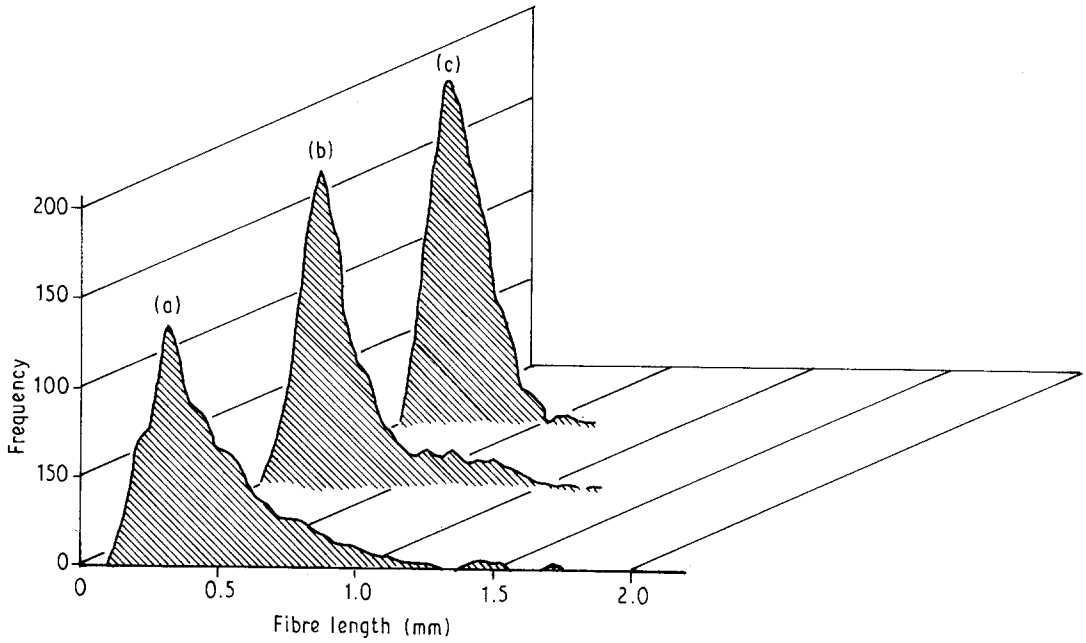

Figure 7 Fibre length distributions for SFRPA50 representing: (a) a granule, (b) a plaque with 0.7 MPa, 6×2 mm^2, (c) a plaque with 0.7 MPa, 6×1 mm^2.

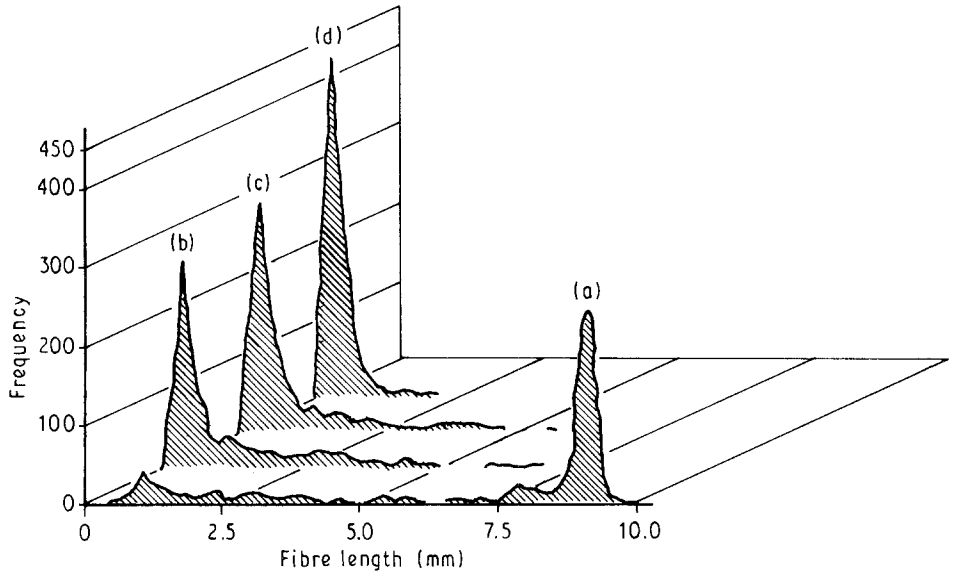

Figure 8 Fibre length distributions for LFRPA50 representing: (a) a granule, (b) a runner with 0.7 MPa (in Fig. 2 the position of the runner sample is shown by ×), (c) a plaque with 0.7 MPa, 6×2 mm^2, (d) a plaque with 1.7 MPa, 6×2 mm^2.

TABLE III Variation of the UTS and elastic modulus with back pressure and gate size

Material	Back pressure (MPa)	Gate size (mm^2)	UTS (MPa)	Elastic modulus (GPa)
SFRPA50	0.7	6×2	195	8.6
SFRPA50	0.7	6×1	186	8.7
SFRPA50	0.7	4×1	184	8.6
SFRPA50	1.7	6×2	193	8.4
LFRPA50	0.7	6×2	208	9.2
LFRPA50	0.7	4×1	191	9.1
LFRPA50	1.7	6×2	198	9.0

the fibres are above the stress-transfer fibre length. Strength, by comparison, is a failure condition where fewer fibres remain above the transfer length. Tolerance of elastic modulus to changes in back pressure and the associated variation in fibre-length distribution has also been shown by Bailey *et al.* [10] for LFRPA50.

4. Conclusions

A criterion for jetting as (die-swell ratio) × (mould-gate depth) ≤ (mould-cavity depth) has a limited application with a gate arrangement where one surface of the gate is flush with the cavity. Jetting depends on fibre content, fibre length, injection ram speed, extent of distortion of the jet upon solidification as well as the ratio of the gate depth to mould-cavity depth. Unfilled and 30% by weight short glass fibre-containing polyamides show no jetting under the injection ram speed/gate size combinations considered here. However, the material becomes extremely prone to jetting

TABLE IV Stress-transfer fibre-length data

Material	Back pressure (MPa)	Gate size (mm^2)	l_{tr} (mm) at strains		% fibres above l_{tr} at strains	
			0.8%	failure	0.8%	failure
SFRPA50	0.7	6 × 2	0.06	0.27	98	45
SFRPA50	0.7	6 × 1	0.06	0.28	96	30
LFRPA50	0.7	6 × 2	0.10	0.48	100	60
LFRPA50	1.7	6 × 2	0.10	0.45	100	40

Values used for l_{tr} determinations: E(fibre) = 69 GPa [9]; τ = 45 MPa [5]; measured fibre diameters of 10 and 17 μm for SFRPA50 and LFRPA50, respectively.

at the higher fibre weight content of 50%, even the long fibre grade in spite of its tendency to swell.

Fibre degradation, as would be expected, gives a narrower fibre-length distribution and reduces the number of fibres above the effective fibre length needed for matrix to fibre stress transfer, particularly at high strains. As a consequence, ultimate tensile strength shows a deterioration, albeit slight, whereas elastic modulus is unaffected.

Acknowledgements

We thank ICI Advanced Materials at Wilton, particularly Dr R. S. Bailey and Dr D. R. Moore for their much valued support and cooperation.

References

1. K. ODA, J. L. WHITE and E. S. CLARK, *Polym. Engng Sci.* **16** (1976) 582.
2. J. A. BRYDSON, "Flow Properties of Polymer Melts" (ILIFFE Books, London, 1970).
3. Y. CHAN, J. L. WHITE and Y. OYANAGI, *J. Rheol.* **22** (1978) 507.
4. R. J. CROWSON and M. J. FOLKES, *Polym. Engng Sci.* **20** (1980) 934.
5. W. H. BOWYER and M. G. BADER, *J. Mater. Sci.* **7** (1972) 1315.
6. J. LUNT, PhD thesis, University of Liverpool (1980).
7. M. AKAY and D. BARKLEY, *J. Mater. Sci.* **26** (1991) 2731.
8. *Idem, Compos. Struct.* **3** (1985) 269.
9. A. H. COTTRELL, "The Mechanical Properties of Matter" (Wiley, New York, 1964).
10. R. S. BAILEY, M. DAVIES and D. R. MOORE, in "Composites Evaluation", edited by J. Herriot (Butterworths, Guildford, 1987) pp. 87–95.

Received 8 August
and accepted 28 November 1991